JOURNAL OF
SYNCHROTRON
RADIATION

ISSN 1600-5775

Received 24 July 2017
Accepted 4 May 2018

Edited by S. M. Heald, Argonne National Laboratory, USA

Keywords: transition-metal oxides; pre-edge peak intensity; temperature dependence; phase transition; XANES.

Rutile- and anatase-type temperature-dependent pre-edge peak intensities in *K*-edge XANES spectra for *A*O (*A* = Mn), A_2O_3 (*A* = Sc, Cr and Mn) and AO_2 (*A* = Ti and V)

Tsubasa Tobase,[a]* Akira Yoshiasa,[a] Tatsuya Hiratoko[a] and Akihiko Nakatsuka[b]

[a]Graduate School of Sciences and Technology, Kumamoto University, Chuoku Kurokami 2-39-1, Kumamoto 860-8555, Japan, and [b]Advanced Materials Science and Engineering, Yamaguchi University, Ube, Yamaguchi 755-8611, Japan. *Correspondence e-mail: tbs.tobase@gmail.com

Pre-edge peaks in 3*d* transition-metal element (Sc, Ti, V, Cr and Mn) *K*-edge XANES (X-ray absorption near-edge structure) spectra in AO_2 (*A* = Ti and V), A_2O_3 (*A* = Sc, Cr and Mn) and *A*O (*A* = Mn) are measured at various temperatures. Quantitative comparisons for the XANES spectra were investigated by using absorption intensity invariant point normalization. The energy position of the difference peak (D peak) is obtained from the difference between the low- and high-temperature XANES spectra. There are two kinds of temperature dependence for pre-edge peak intensity: rutile- and anatase-type. The true temperature dependence of a transition to each orbital is obtained from the difference spectrum. In both anatase and rutile, the pre-edge peak positions of A2 and A3 are clearly different from the D1- and D2-peak positions. The A1 peak-top energies in both phases of VO_2 differ from the D1 peak-top energies. The D-peak energy position determined by the difference spectrum should represent one of the true energies for the transition to an independent orbital. The peak-top positions for pre-edge peaks in XANES do not always represent the true energy for independent transitions to orbitals because several orbital transitions overlap with similar energies. This work suggests that deformation vibration (bending mode) is effective in determining the temperature dependence for the D-peak intensity.

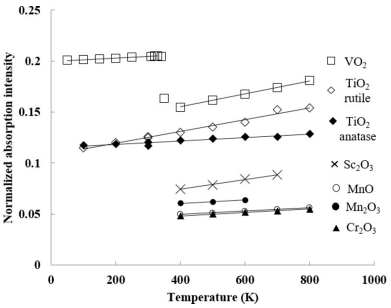

1. Introduction

X-ray absorption near-edge structure (XANES) provides information about local structures around an X-ray absorbing atom. The pre-edge peaks appear at the *K*-edge of transition-metal elements (de Groot *et al.*, 1989) and these peaks are located several electronvolts before the main absorption edge. The pre-edge features of transition-metal elements are related to the coordination number, oxidation state and the point symmetry of the absorbing atom (Yamamoto, 2008).

Temperature dependencies on the pre-edge peak intensity have been observed in various compounds (Bridges *et al.*, 2000; Durmeyer *et al.*, 2010; Hashimoto *et al.*, 2007; Hiratoko *et al.*, 2013; Manuel *et al.*, 2012; Sato *et al.*, 2005). Hiratoko *et al.* (2013) quantified the linear dependence of Ti pre-edge peak features in a variety of compounds over a large temperature range. The Ti sites in TiO_2 rutile and anatase have the same point symmetry. It is known that the A1 and A2 peaks in rutile-type TiO_2 show clear temperature dependence, while it is known that there is no temperature dependence for the A3 peak (Durmeyer *et al.*, 1990, 2010). The temperature dependence of pre-edge peaks in the Ti *K*-edge XANES spectra showed different tendencies which is also a result of harmonic

https://doi.org/10.1107/S1600577518006902

thermal vibration. However, a sufficient comparative study and detailed interpretation of the temperature dependence of pre-edge peak intensity over a wide temperature region has yet to be conducted in several transition-metal oxides.

Several XANES studies have been carried out to investigate the mechanism of the ferroelectric–dielectric phase transition in $BaTiO_3$ and $PbTiO_3$ (Balzarottie *et al.*, 1980; Miyanaga *et al.*, 2002; Ravel & Stern, 1995; Sato *et al.*, 2005; Sicron *et al.*, 1994; Yoshiasa *et al.*, 2016). Many researchers (Balzarottie *et al.*, 1980; Miyanaga *et al.*, 2002; Ravel & Stern, 1995; Sato *et al.*, 2005; Sicron *et al.*, 1994; Yoshiasa *et al.*, 2016) have clarified that the Ti ion occupies an off-center position in the distorted TiO_6 octahedral site, the geometric distortion of the tetragonal phase decreases with increasing temperature and the A2 pre-edge peak intensity decreases characteristically. These results showed that the A2 pre-edge peak intensity in the ferroelectric phase depends on the degree of distortion around the Ti atoms. Other titanium compounds have characteristic features in pre-edge peaks (Pillep *et al.*, 1997; Waychunas, 1987).

In this article, we quantified the behavior of each metal pre-edge peak in transition-metal oxides (Sc_2O_3, TiO_2, VO_2, Cr_2O_3, MnO and Mn_2O_3) over a large temperature range and investigated how the intensity of the pre-edge peak feature changes with temperature. Here we will show that the temperature dependence of pre-edge peak intensities for $1s \rightarrow t_{2g}$ can be classified into the TiO_2 rutile or anatase types. Pre-edge peaks can be divided in more detail from the temperature dependence of the XANES spectra. We emphasize from our observation of temperature dependence that the difference-peak (D peak) positions represent the transition energies rather than simple pre-edge peaks.

2. Experimental

TiO_2 rutile and anatase are the same specimens as used by Hiratoko *et al.* (2013). All specimens [Sc_2O_3 (99.9%), VO_2 (99.5%), Cr_2O_3 (99.9%), MnO (99.9%) and α-Mn_2O_3 (99.9%)] were commercially available (Furu-uchi Chemical Co. Ltd) and were examined by X-ray diffraction methods. Appropriate amounts of fine-powder sample and boron nitride powder were mixed and pressed into pellets of <0.2 mm thickness and 10.0 mm diameter. Adjusting the sample content allowed all samples to show edge-jumps of $0.7(\Delta\mu d)$, where μ is the linear absorption coefficient and d is the sample thickness. The Sc, Ti, V, Cr and Mn *K*-edge XANES were measured in transmission mode at beamline BL-9C of the Photon Factory at the High Energy Accelerator Research Organization (KEK), Tsukuba, Japan. Synchrotron radiation was monochromated by a Si(111) double-crystal monochromator. X-ray energy calibration was performed by setting the copper metal pre-edge absorption peak to 8978.8 eV. Mirrors were used to eliminate higher harmonics. X-ray absorption measurements in the temperature range 300–900 K were performed under a helium atmosphere.

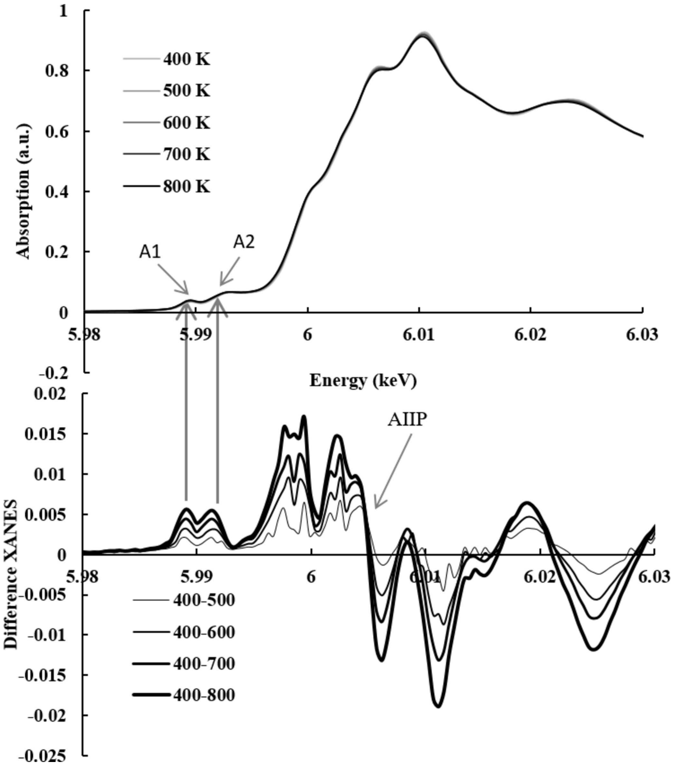

Figure 1
Cr *K*-edge XANES spectra of Cr_2O_3 at various temperatures.

In order to clarify temperature dependence, we plotted the difference spectrum between the low-temperature (400 K) and high-temperature spectra. We found the existence of an energy point where the intensity does not change with temperature, near each absorption edge for all samples. This point is called the absorption intensity invariant point (AIIP), *i.e.* an energy point at which the intensity does not change with temperature (Hiratoko *et al.*, 2013). The arrow marked AIIP indicates the AIIP in Fig. 1. The physical meaning of the AIIP will be regarded as an extension of the EXAFS baseline. Using the AIIP peak intensity as a standard point, it is possible to present a quantitative comparison of the pre-edge peaks in various compounds over a wide temperature range. We normalized the spectrum intensity for the samples so that the intensity at the AIIP is 1.0 and compared the temperature dependence of the XANES pre-edge peaks among the samples. The AIIP-based normalization allows the elimination of errors caused by the reference point itself changing with temperature. XANES amplitudes at energies higher than the AIIP dampen with increasing temperature as a result of Debye–Waller type effects (Hiratoko *et al.*, 2013). The standardization using the AIIP is effective when comparing the temperature dependence of absolute intensity in the XANES spectra for various compounds.

3. Results and discussion

3.1. AIIP-based normalization and temperature dependence of XANES features

In every case, the AIIP is observed near each absorption edge for all samples. Fig. 1 shows an example of a Cr *K*-edge

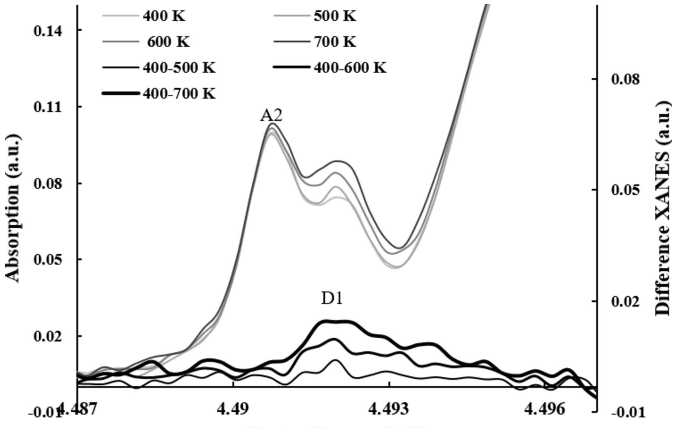

Figure 2
Sc K-edge XANES spectra of Sc_2O_3 at various temperatures.

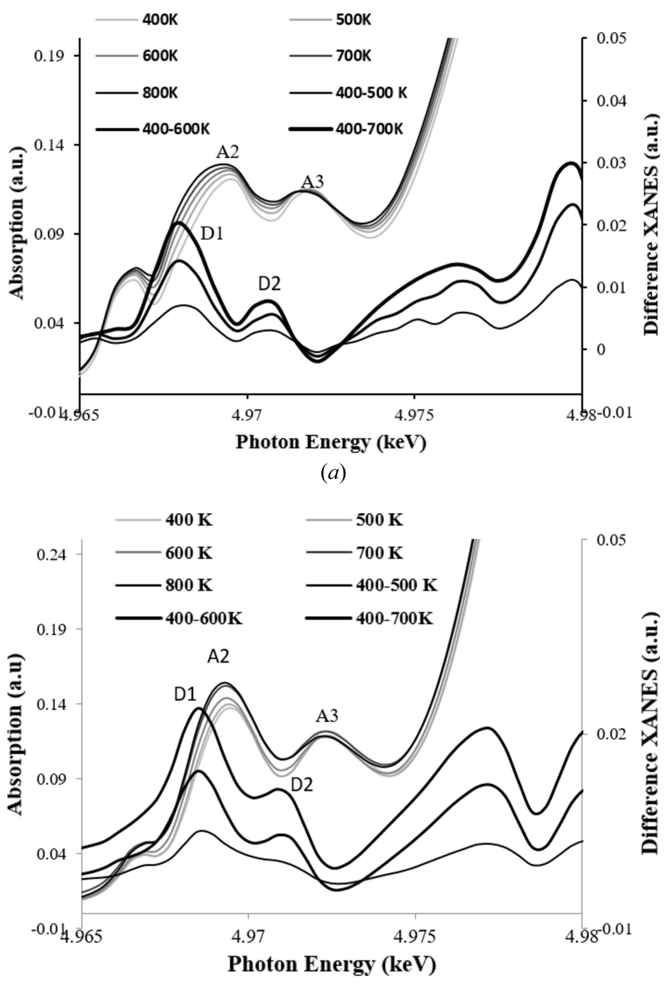

(*a*)

(*b*)

Figure 3
Ti K-edge XANES spectra of TiO_2 anatase (*a*) and rutile (*b*) at various temperatures.

XANES spectrum of C_2O_3 in the range 400–800 K (AIIP energy: 6005.3 eV) and the difference between the spectra at 400 K and those at higher temperatures (600–800 K). XANES amplitudes are clearly seen to dampen at energies higher than the AIIP owing to the Debye–Waller factor effect at higher temperatures; the line displays the attenuation of a sine curve. Conversely, amplitudes increase with temperature at energies lower than the AIIP for several peaks in the difference spectra. Figs. 2–7 show the pre-edge region in the XANES spectra for each sample and the difference spectra between the lower and higher temperatures. The energy positions of the D1 and D2 peaks are obtained from the difference spectra, *i.e.* the difference between the low- and high-temperature spectra (lower section of each figure).

3.1.1. Temperature dependence of Sc_2O_3 and TiO_2. Fig. 2 shows the Sc K-edge XANES spectra for Sc_2O_3 at various temperatures. Two clear pre-edge peaks are observed; we have labelled them as A1 and A2 for each peak of the pre-edge region. The A1 peak is assigned to the transition $1s \rightarrow 3d$ described by Bart (1986). The intensity of the A2 pre-edge peak has a large temperature dependence whereas a temperature dependence for the A1 pre-edge peak is not observed.

Figs. 3(*a*) and 3(*b*) represent the Ti K-edge XANES spectra in anatase and rutile at 400–800 K, and the difference between the spectra at 400 K and those at higher temperatures (500–800 K). The A3 pre-edge peak has no temperature dependence and the difference spectra have no magnitude in either compound. This tendency is similar to the A1 peak in Sc_2O_3. It is important that the zero-value position in the difference spectra and A3-peak position are not identical. In both anatase and rutile, the pre-edge peak positions of A2 and A3 are clearly different from the peak positions of the difference spectra. We have labelled them as D1 and D2 at the top of each peak. The features of the difference spectra for rutile and anatase are similar, though each pre-edge feature in the XANES spectra is significantly different. The D2 positions correspond to the col between the A2 and A3 peaks. We have reported that the A2 pre-edge peaks in both compounds indicate different temperature dependencies. The peaks are formed from transitions between orbitals. The temperature dependence of the transition to each orbital is different, and these transitions can be separated by preparing difference spectra. The true temperature dependence of a transition to an orbital is obtained from the difference spectra. The A2 peak shifts to a lower energy at higher temperatures. The origin of the peak shift can be explained by the peak position and increase in the D1 peak in the difference spectra.

3.1.2. Pre-edge features and phase transitions in VO_2. Figs. 4(*a*) and 4(*b*) show the V K-edge XANES spectra of the VO_2 monoclinic phase at 50–250 K and of the VO_2 tetragonal phase at 400–700 K. VO_2 undergoes structural phase transitions from monoclinic to tetragonal at 340 K. There is a clear change in pre-edge shape between monoclinic and tetragonal phases (Figs. 4*a* and 4*b*). Pre-edge peaks are observed in both phases with temperature dependencies. In Fig. 4, the A1 peak at 5467 eV is a result of the $1s \rightarrow t_{2g}$ transition by comparison of the edge structure with the calculated density state of the conduction band in the VO_2 tetragonal phase (Bianconi, 1982; Gupta *et al.*, 1977). The absorption intensity of the A2 peak in the low-temperature monoclinic phase decreases discontinuously at the transition point, but no energy shift for this peak is

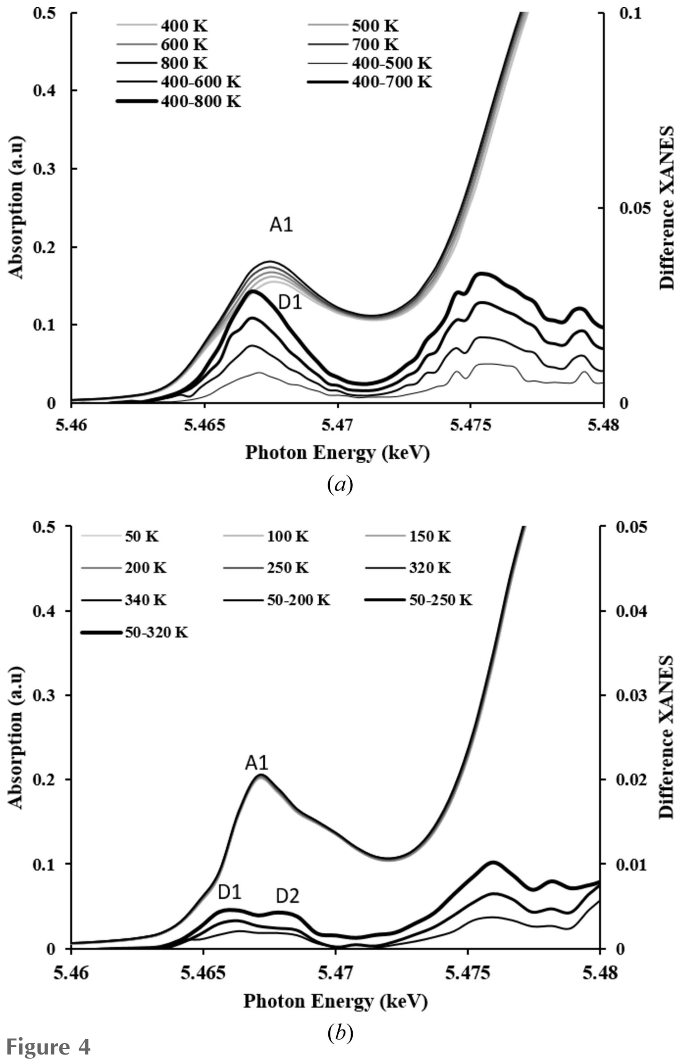

(*a*)

(*b*)

Figure 4
V *K*-edge XANES spectra of VO_2 tetragonal (*a*) and monoclinic (*b*) phases at various temperatures.

observed between the monoclinic and tetragonal phases. The A1 peak will also be assigned as the $1s \rightarrow t_{2g}$ transition in the monoclinic phase. The features of the difference spectra or both low- and high-temperature phases are different although one clear peak is observed in the XANES spectrum. We labelled the peaks in the difference spectra as D1 and D2 for the low-temperature phase. The A1 peak-top energies in both phases are different from the D1 or D2 peak-top energies.

3.1.3. Temperature dependence in Cr_2O_3, Mn_2O_3 and MnO

Fig. 5 shows the Cr *K*-edge XANES spectra of Cr_2O_3 at various temperatures. The A1 initial pre-edge peak is thought to correspond to a transition to the lowest unoccupied molecular orbital. The A1 and A2 peaks are assigned to the $1s \rightarrow t_{2g}$ transition and the $1s \rightarrow e_g$ transition, respectively, as reported by Grunes (1983). Both A1 and A2 peaks in Cr_2O_3 have the same temperature dependencies, although the peak heights are different. The energy positions of the D1 and D2 peaks, which are obtained from the difference spectra between the low- and high-temperature spectra, are different from the peak tops of the A1 and A2 pre-edge peak positions and are located just before the peak top in the XANES spectra.

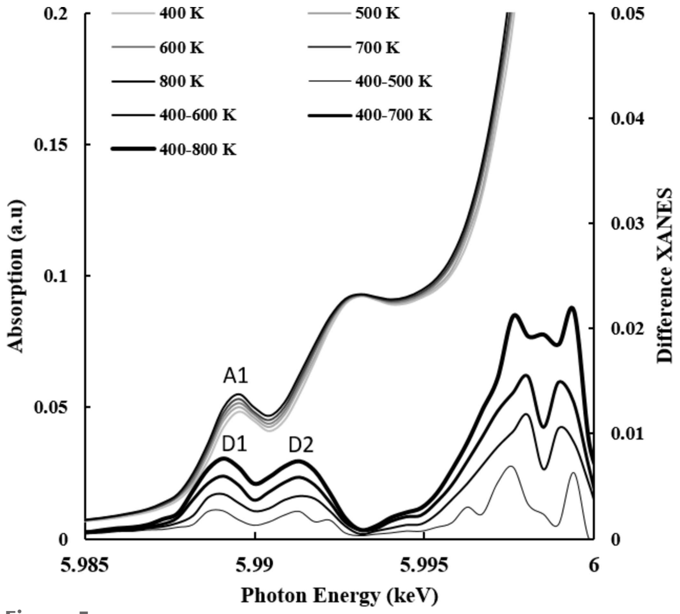

Figure 5
Cr *K*-edge XANES spectra of Cr_2O_3 at various temperatures.

Figs. 6 and 7 show the Mn *K*-edge XANES spectra of Mn_2O_3 and MnO at various temperatures. S1 is an acronym for the pre-shoulder. A clear pre-edge peak is not observed, though several peaks were distinguishable in the difference spectra between the low and high temperatures. Peaks are obtained from the temperature dependence of the pre-shoulder, and the energy value of the electron orbital can be determined.

3.2. Increase of pre-edge intensity and gradient against temperature

3.2.1. Temperature gradient for the A pre-edge peak intensity

Since AIIP-based normalization can eliminate errors due to the fact that the reference point itself changes with temperature, it is possible to compare the intensities of different compounds. Fig. 8 shows the absorption intensity of the pre-edge peak or pre-shoulder in the metal *K*-edge XANES spectra *versus* temperature (*i.e.* the A2 peak in Sc_2O_3, the A2 peak in TiO_2, the A1 peak in VO_2, the A1 peak in Cr_2O_3, S1 in Mn_2O_3 and S1 in MnO).

Table 1 shows the energy and temperature gradient of the peak intensity for the pre-edge peak, pre-shoulder and D peak in each compound. The A1 peak in the VO_2 tetragonal phase and the A2 peak in Sc_2O_3 have temperature gradients of 0.0071 and 0.0048 (intensity/100 K), respectively. The gradient is similar to A2 of TiO_2 rutile, attributed to the $1s \rightarrow t_{2g}$ transition. On the other hand, the A1 pre-edge peak of the VO_2 monoclinic phase has the same temperature dependence as the A2 peak in TiO_2 anatase. The difference in the temperature dependence of the pre-edge peaks of the monoclinic and tetragonal phases should indicate that the vibrational character is changed by the difference in local coordination environments. The rate of increase of the A2 pre-edge peak intensity in Sc_2O_3, A2 in TiO_2 rutile and A1 in the VO_2 tetragonal phase are large compared with the rest of

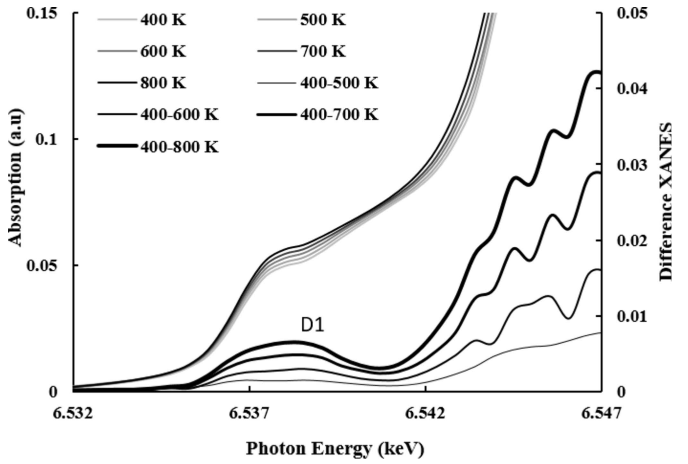

Figure 6
Mn *K*-edge XANES spectra of Mn_2O_3 at various temperatures.

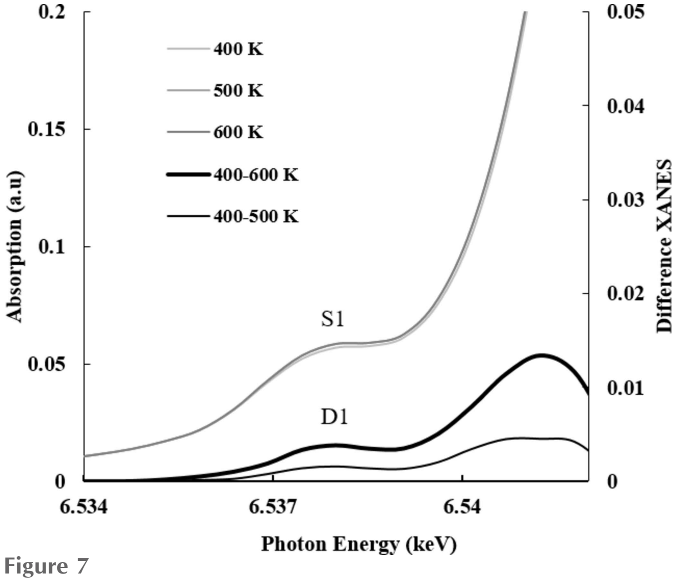

Figure 7
Mn *K*-edge XANES spectra of MnO at various temperatures.

the samples. Although the height of the A1 peak in the VO_2 monoclinic phase is obviously higher than those for A1 in the VO_2 tetragonal phase and for A2 in Sc_2O_3, the temperature gradient of A1 in the VO_2 monoclinic phase is clearly low like A2 in TiO_2 anatase. The temperature dependence of the pre-edge peak is not directly related to pre-edge peak heights. Large temperature gradients are seen in low peak intensities.

The temperature dependence of a transition to each orbital is different. Temperature dependence is not observed in the pre-edge peak for a $1s \rightarrow e_g$ transition. The temperature dependence is permitted only in the pre-edge peaks assigned to the $1s \rightarrow t_{2g}$ transition. The dipole transition has no temperature dependence. A large temperature dependence occurs in the mixture of the quadrupole and dipole transitions. The hybridization between cations and oxygen is important in each compound. Hiratoko *et al.* (2013) succeeded in the quantitative study of the temperature dependence of pre-edge peaks intensity in various titanium compounds. There were two kinds of temperature dependences in the pre-edge peaks that are assigned to a mixture of the quadrupole and dipole transitions (rutile- and anatase-type). The gradient of the A2 peak intensity for TiO_2 rutile is similar to the gradient of A1 in the VO_2 tetragonal phase and A2 in Sc_2O_3. There is a possibility that the high pre-edge peaks with large gradient in Sc_2O_3 and VO_2 are composed of the same transitions in TiO_2 rutile. The transition is a mixture of the quadrupole and dipole transitions.

Table 1
Slope and energy of peak intensity for the A pre-edge and D peaks in each compound.

Compound	Peak labels	Energy (eV)	Slope of peak intensity for A or D peak (intensity/100K)	Number of 3*d* electrons
Sc_2O_3	A2 and D1	4491.97	0.0048	0
TiO_2 rutile	A2	4969.27	0.0063	0
	D1	4968.47	0.0074	
	D2	4970.87	0.0035	
TiO_2 anatase	A2	4969.65	0.0016	0
	D1	4967.85	0.0067	
	D2	4970.85	0.0025	
VO_2 tetragonal	A1	5467.05	0.0069	1
	D1	5466.68	0.0071	
VO_2 monoclinic	A1	5467.05	0.0015	
	D1	5466.31	0.0015	
Cr_2O_3	A1	5989.53	0.0016	3
	D1	5989.08	0.0018	
	D2	5991.32	0.0017	
Mn_2O_3	S1 and D1	6537.99	0.0014	4
MnO	S1 and D2	6537.99	0.0017	5

3.2.2. Temperature gradient for D peaks in different spectra and deformation vibration

It is known that the pre-edge peak intensity increase is usually linear with increasing temperature by harmonic thermal vibration (Hiratoko *et al.*, 2013). On the other hand, the negative peaks in the difference spectra were identified and observed only in the Ti and Zr *K*-edges for para- and ferroelectric $PbZrO_3$, $PbTiO_3$ and $BaTiO_3$

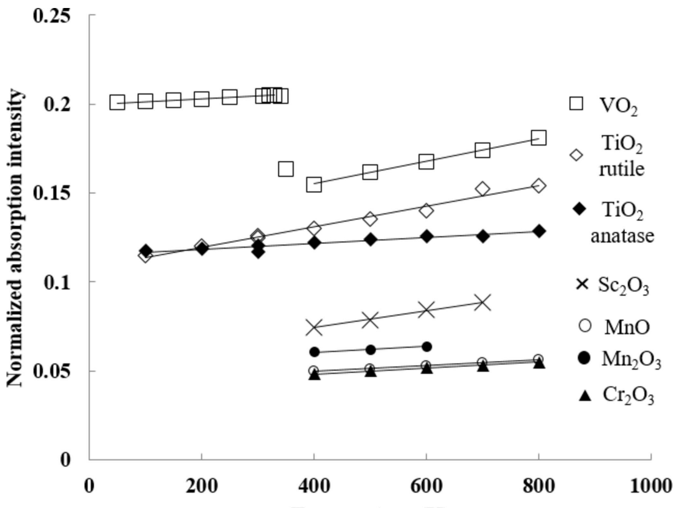

Figure 8
Temperature dependence of normalized absorption intensity of the pre-edge peak or pre-shoulder of metal *K*-edge features for several samples (*i.e.* A2 peak in Sc_2O_3, A2 peak in TiO_2, A1 peak in VO_2, A1 peak in Cr_2O_3, S1 in Mn_2O_3 and S1 in MnO).

(Balzarottie *et al.*, 1980; Miyanaga *et al.*, 2002; Ravel & Stern, 1995; Sato *et al.*, 2005; Sicron *et al.*, 1994; Yoshiasa *et al.*, 2016). The decrease of pre-edge peak intensity is speculated because of the shift from the off-center position of the Ti and Zr atom, with respect to the oxygen octahedron, to the center position. Deformation vibration (bending mode) in thermal vibration is also effective in determining the temperature dependence of the peak intensity. It is considered that a correlation between the pre-edge peak intensity and the mean-square relative displacement (MSRD) would not be observed because the MSRD of the EXAFS Debye–Waller factor influences mainly stretching vibrations.

Many materials have been studied using pre-edge peaks in XANES. The temperature gradients for the A2 peak in XANES spectra of anatase and rutile are 0.0016 (intensity/100 K) and 0.0063 (intensity/100 K), respectively. The correct slope for each D peak is shown in Table 1. The temperature gradients for the D1 peak in anatase and rutile are 0.0067 and 0.0074 (intensity/100 K), respectively. It is important to show that the D1 transition with a large temperature dependence exists in anatase. The peak-top position for pre-edge peaks in XANES does not always represent the true energy for independent transitions to different orbitals because several orbital transitions with similar energies overlap. The D-peak energy position, which is determined by the difference spectra, should represent one of the true energies for the transition to an independent orbital. It is also shown that the temperature dependence of the pre-edge peak intensity depends not only on the characteristics of the electron orbital but also on the difference in overlapping of the electron orbitals.

4. Conclusions

The true energy positions for transitions to independent orbitals in XANES spectra of transition-metal oxides were obtained from the difference spectra (D peaks). Many individual studies have been made on these useful materials. Here, we show common observations in the compounds of first-row transition-metal elements.

We usually use one copper pre-edge to calibrate the X-ray energy. In XAFS experiments, errors are included in determining the absolute value of the observed energy coming from the *d*-space value of the monochromator crystal and the setting conditions. The X-ray energy resolution is also different for each device. Each pre-edge peak is a superposition of several electron orbitals with slightly different energy values. The symmetry of the occupying site, which is defined crystallographically, may differ locally from those assuming three-dimensional periodicity. The energy values of the orbitals shifted several electronvolts depending on the chemical bonding and local structure. There are many theoretical calculations that attempt to reproduce the shape of the pre-edge, and the energy values of each electron orbital have been optimized in the simulations. Fitting with the experimental value is necessary to confirm the validity of the model (with some approximation) adopted for calculation. Here, it could be suggested that the D peak represents the transition energy of the electron orbital rather than the simple pre-edge peak. From an experimental point of view, we would like to suggest development by experts in theory and simulation. We also expect that the temperature dependence of absorption intensity for each orbital should be verified by future simulations. The correct orbital temperature dependence was indicated by each D peak of Table 1. There were roughly two types of temperature dependence. The essence of this should be clarified by theory. We propose that AIIP-based normalization is the best method from experimental observations over a wide temperature range. Although there were small errors in the AIIP, we could perform more accurate temperature-dependence experiments using AIIP.

Funding information

This study was performed within the Photon Factory Project PAC No. 2012G530, 2014G534 and 2014G535. This work was supported by JSPS Grant-in-Aid for JSPS Research Fellow JP16J10062.

References

Balzarotti, A., Comin, F., Incoccia, L., Piacentini, M., Mobilio, S. & Savoia, A. (1980). *Solid State Commun.* **35**, 145–149.
Bart, J. C. J. (1986). *Adv. Catal.* **34**, 203.
Bianconi, A. (1982). *Phys. Rev. B*, **26**, 2741–2747.
Bridges, F., Booth, C. H., Kwei, G. H., Neumeier, J. J. & Sawatzky, G. A. (2000). *Phys. Rev. B*, **61**, R9237–R9240.
Durmeyer, O., Beaurepaire, E., Kappler, J. P., Brouder, Ch. & Baudelet, F. (2010). *J. Phys. Condens. Matter*, **22**, 125504.
Durmeyer, O., Kappler, J. P., Beaurepaire, E., Heintz, J. M. & Drillon, M. J. (1990). *J. Phys. Condens. Matter*, **2**, 6127–6136.
Groot, F. M. F. de, Grioni, M., Fuggle, J. C., Ghijsen, J., Sawatzky, G. A. & Petersen, H. (1989). *Phys. Rev. B*, **40**, 5715–5723.
Grunes, L. A. (1983). *Phys. Rev. B*, **27**, 2111–2131.
Gupta, M., Freeman, A. J. & Ellis, D. E. (1977). *Phys. Rev. B*, **24**, 4406.
Hashimoto, T., Yoshiasa, A., Okube, M., Okudera, H. & Nakatsuka, A. (2007). *AIP Conf. Proc.* **882**, 428–430.
Hiratoko, T., Yoshiasa, A., Nakatani, T., Okube, M., Nakatsuka, A. & Sugiyama, K. (2013). *J. Synchrotron Rad.* **20**, 641–643.
Manuel, D., Cabaret, D., Brouder, C., Sainctavit, P., Bordage, A. & Trcera, N. (2012). *Phys. Rev. B*, **85**, 224108.
Miyanaga, T., Diop, D., Ikeda, S. & Kon, H. (2002). *Ferroelectrics*, **206**, 407.
Pillep, B., Fröba, M., Phillips, M. L. F., Wong, J., Stucky, G. D. & Behrens, P. (1997). *Solid State Commun.* **103**, 203–207.
Ravel, B. & Stern, E. A. (1995). *Physica B*, **208–209**, 316–318.
Sato, K., Miyanaga, T., Ikeda, S. & Diop, D. (2005). *Phys. Scr.* T**115**, 359–361.
Sicron, N., Ravel, B., Yacoby, Y., Stern, E. A., Dogan, F. & Rehr, J. J. (1994). *Phys. Rev. B*, **50**, 13168–13180.
Waychunas, G. A. (1987). *Am. Miner.* **72**, 89–101.
Yamamoto, T. (2008). *X-ray Spectrom.* **37**, 572–584.
Yoshiasa, A., Nakatani, T., Hiratoko, T., Tobase, T., Nakatsuka, A., Okube, M., Arima, H. & Sugiyama, K. (2016). *J. Phys. Conf. Ser.* **712**, 012121.